

Kondo-transport spectroscopy of single molecule magnets

C. Romelike⁽¹⁾, M. R. Wegewijs⁽¹⁾, W. Hofstetter⁽²⁾, and H. Schoeller⁽¹⁾

(1) Institut für Theoretische Physik A, RWTH Aachen, 52056 Aachen, Germany

(2) Institut für Theoretische Physik, J. W. Goethe-Universität Frankfurt, 60438 Frankfurt am Main, Germany

We demonstrate that in a single molecule magnet (SMM) strongly coupled to electrodes the Kondo effect involves all magnetic excitations. This Kondo effect is induced by the quantum tunneling of the magnetic moment (QTM). Importantly, the Kondo temperature T_K can be much larger than the magnetic splittings. We find a strong modulation of the Kondo effect as function of the transverse anisotropy parameter or a longitudinal magnetic field. For both integer and half-integer spin this can be used for an accurate transport spectroscopy of the magnetic states in low magnetic fields on the order of the easy-axis anisotropy parameter. We set up a relationship between the Kondo effects for successive integer and half-integer spins.

PACS numbers: 72.10.Fk, 75.10.Jm, 75.30.Gw, 75.60.Jk

Introduction. Single molecule magnets (SMMs) allow the study of quantum phenomena on a mesoscopic scale, namely the quantum tunneling of the magnetic moment. SMMs such as Mn_{12} or Fe_8 have attracted intense experimental and theoretical investigation [1] in recent years. Due to weak intermolecular interaction molecular crystal properties can be assigned to single molecules described by a large spin ($S > 1/2$), and easy-axis and transverse anisotropies. Recently, two groups [2, 3] have trapped a single molecule magnet (Mn_{12}) in a three-terminal transport setup and measured transport through the single molecule. Electron transport fingerprints due to both sequential [2, 3] and inelastic co-tunneling [3] processes were observed and associated with the molecular magnetic states. Theoretical works [4, 5, 6] predicted that fingerprints of magnetic quantum tunneling (QTM) can in principle be identified in transport measurements in the charge (sequential tunneling) as well as in the spin-actuation (Kondo) regime. Especially the latter regime of strong coupling to the electrodes is of importance since the Kondo effect shows up as a sharp zero-bias anomaly with width given by the Kondo temperature T_K . The Kondo effect has been observed experimentally in many other systems with small spins (e.g. quantum dots [7, 8, 9, 10, 11] and single molecules [12, 13]). For SMMs with half-integer spin S in zero magnetic field it was shown [5] that the Kondo effect arises from a cooperation of both spin exchange processes with the reservoirs and the intrinsic tunneling of the magnetic moment. The strong coupling fixed point is of pseudo-spin-1/2 type. In this limit the exchange coupling J is weak, such that the resulting Kondo temperature $T_K(J; \dots)$, where $\dots \sim 1$ meV is the scale of the anisotropy splittings between the magnetic states. In this case, the Kondo effect involves only the two magnetic ground states of the SMM and does not occur for integer spin.

In this Letter we study the Kondo effect in the experimentally more favorable regime of strong exchange ($J \sim 0.1$ eV) where the Kondo temperature becomes larger than the magnetic splittings $T_K(J; \dots)$. We find that excited magnetic levels on the SMM, belonging to different topological sectors (with respect to rotations

around the z-axis), become essentially involved in the Kondo effect. In zero magnetic field and for half-integer spin the Kondo effect can be modulated by changing the transverse anisotropy, resulting in a sequence of Kondo effects associated with different magnetic excited states. A longitudinal magnetic field can induce two important new effects: (1) For both integer and half-integer spin the Kondo effect is suppressed at each anticrossing of magnetic levels belonging to the same topological sector. The corresponding sharp magnetic field scale is determined by the transverse magnetic anisotropy. Therefore the study of the magnetic field dependence allows for an accurate spectroscopy of the magnetic states. This modulation of the Kondo effect allows for an experimental proof of the existence of QTM in a single molecule in a transport junction and to determine the important microscopic parameters characterizing the SMM in that setup. The magnetic field induced Kondo effect for integer spin SMMs allows many molecular magnets like e.g. Fe_8 to be studied without charging the molecule to obtain a half-integer spin. (2) We find that the Kondo effects for successive integer and half-integer spin S display a close correspondence when shifted in magnetic field energy by the easy-axis anisotropy parameter D .

Model. We consider a SMM (Fig. 1) in a transport setup where the applied voltages, charging effects and low temperature suppress single-electron processes [5]. In the presence of a longitudinal magnetic field the Hamiltonian reads $H = H_{SMM} + H_{ex} + H_{res}$:

$$H_{SMM} = D S_z^2 + \frac{1}{2} B_2 S_+^2 + S^2 + H_z S_z \quad (1)$$

$$H_{ex} = \sum_X J S \cdot s \quad (2)$$

$$H_{res} = \sum_k a_k^\dagger a_k \quad (3)$$

where S_z is the projection of the SMM's spin on the easy z-axis, and $S = S_x + i S_y$. The terms in Eq. (1) describe, respectively, the easy-axis magnetic anisotropy of the molecule, the transverse anisotropy perturbation and the coupling to a magnetic field (H_z) along the easy axis. The g-factors are absorbed into the magnetic field. For simplicity we have taken a 2-fold rotation-symmetry

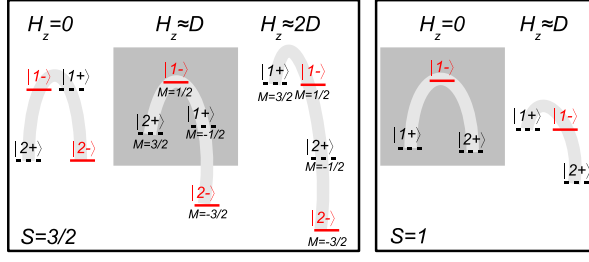


FIG. 1: Energy diagram for H_M with $B_2 = D$ without (left) and with (right) magnetic field. The two subsets of eigenstates of different magnetic symmetry are indicated by full and dashed bars.

axis, which is dominant in many molecular magnets. The Hilbert space of H_{SM} is split into two disjoint topological subspaces since the 2-fold rotational symmetry about the z -axis is preserved under the longitudinal magnetic field. While for half-integer S these spaces are spanned by an equal number of $n_+ = n_- = S + 1 = 2$ basis-states $f\beta; M_{\text{eq}} = S; (S-2); \dots; (S-3); (S-1)$, for integer spin they are spanned by $n_+ = S + 1$ states $f\beta; M_{\text{eq}} = S; S+2; \dots; S-2; S$ for $\beta = +$ and by $n_- = S$ states $f\beta; M_{\text{eq}} = S+1; S+3; \dots; S-3; S-1$ for $\beta = -$. The eigenstates $j_l i$ of H_{SM} with energies E_l are labeled by $l = 1; 2; \dots; n$ in order of decreasing energy in each subspace (see Fig. 1). Eq. (2) describes the exchange coupling of the molecular spin to the effective reservoir Eq. (3) (bandwidth $2W$ and constant density of states ρ). The electronic states are labeled by k and denote the even combination of left and right physical electrode states [4, 15]. The local electron spin in the reservoir is $s = \sum_{kk'} a_{k0}^\dagger \sigma_k a_{k0} = 2$ where σ is the Pauli matrix vector. The exchange coupling J is induced by virtual electron tunneling processes and is antiferromagnetic due to the strong energy- and charge quantization effects. The Kondo spin-scattering of conduction electrons on the SMM transfers charge between physical left and right electrodes and can resonantly enhance the linear conductance. The halfwidth at halfmaximum of the resulting zero-bias differential conductance peak at $T = 0$ is the Kondo temperature T_K .

For a qualitative discussion it is useful to change to the exact representation of Eq. (2) in the eigenbasis of the molecular states $j_l i$:

$$H_{\text{ex}} = \sum_{l=0}^N \sum_{i=x,y} \sum_{j=1}^n J_{1l0}^i P_{1l0}^i S_i + \sum_{j=1}^n J_{1l0}^z j_l i h_l^0 j_s z A : (4)$$

The Hamiltonian Eq. (4) describes the exchange processes involving reservoir electrons and internal magnetic degrees of freedom of the SMM. This projection makes explicit that the QTM parameter B_2 and the external magnetic field H_z modulate the effective couplings through the matrix elements of the molecular spin operator S . The first, transverse, term describes the spin-scattering involving a pair of states $j_l i$ and

$j_l^0 i$ in terms of pseudo-spin-1/2 operators $P_{1l0}^x; i P_{1l0}^y = (j_l i h_l^0 - j_l^0 i h_l^0) / 2$ with effective exchange couplings

$$J_{1l0}^{x=y} = J h_l i \beta_+ - S j_l^0 i : (5)$$

In total, there are $n_+ n_-$ such pairs of states from opposite topological sectors. The longitudinal couplings read $J_{1l0}^z = J h_l i \beta_z j_l^0 i$. Longitudinal spin operators $P_{1l0}^z = (j_l i h_l^0 + j_l^0 i h_l^0) / 2$ can only be introduced in a unique way if an approximate projection onto a single pair is made. For instance, one recovers the projection of Ref. [5] onto the ground state pair for zero-field and half-integer S by using time-reversal symmetry and by truncating the excited states. However, such a truncation is not valid in the regime of interest here: the strong exchange coupling J gives rise to a Kondo temperature that can be larger than the magnetic splittings ($T_K \sim 2SD$ for $B_2 = D$). The Kondo effect can occur irrespective of whether the pair of states $j_l i$ and $j_l^0 i$ are ground- or excited states of the SMM and whether they are exactly degenerate or not. The Kondo effect therefore involves contributions from multiple topological pairs. This we confirm explicitly by calculating the projection of the full many-body ground state onto each molecular eigenstate using the NRG. Thus the full expression for H_{ex} , Eq. (4), must be retained for which a unique decomposition into a sum of independent pairs is not possible. This is due to the fact that a single eigenstate of the SMM $j_l i$ is paired with $n_- > 2$ states $j_l^0 i$.

Physical picture. Variation of either the QTM parameter B_2 or the magnetic field H_z results in anticrossings of magnetic levels. As shown in Fig. 1 the variation of the magnetic field leads to an alternating sequence of degeneracies between pairs of levels which are in different subspaces (crossings) or in the same subspace (anticrossing). Importantly, this occurs in the low magnetic field energy window where the Zeeman splittings are still smaller than T_K ($E_l - E_{l^0} < T_K$). The effective couplings in Eq. (4) are modulated strongly at each anticrossing leading to a suppression of the Kondo effect on a scale B_2 , as we now explain. At an anticrossing states $j_l i$ and $j_l^0 i$ from the same topological sector are close in energy and strongly hybridize due to the transverse anisotropy. Following two levels adiabatically during an anticrossing they interchange their role and one basis state picks up a relative phase. For example, in Fig. 1 the level $j_l i$ is moving upwards and the level $j_l^0 i$ downwards in energy after the anticrossing. For each topological pair involving one of the anticrossing levels this leads to a sign change of one of the transverse couplings, as can be seen easily from Eq. (5). The latter therefore vanish at the anticrossing and the Kondo effect is expected to be suppressed. This happens on a magnetic field scale proportional to the tunnel splitting, i.e. will occur as a sharp feature in the linear conductance as function of a longitudinal magnetic field. In a similar way, in zero field the variation of the QTM parameter B_2 itself leads to a series of

anticrossings, which for a half-integer spin preserves the 2-fold Kramers degeneracy of all levels. This happens due to the non-uniform level spacing and the coupling of states occurs in different orders of perturbation theory in B_2 (higher-lying levels hybridize more strongly for weak B_2).

Method. We use Wilson's NRG [16, 17] to treat non-perturbatively the full model $H = H_{\text{SMM}} + H_{\text{ex}} + H_{\text{res}}$. As NRG input parameters we use number of states $N = 1000$, discretization $\omega = 2$ and $D = 5 \cdot 10^{-5}W$. We analyzed the NRG level flow as function of iteration number N_{iter} in order to determine the low-temperature fixed point for $H_z = 0$. The Kondo temperature is defined as the energy scale where the crossover to strong coupling takes place. We also calculated the spectral function within the T-matrix approach [18]: $A(\omega) = \frac{1}{\pi} \text{Im} T(\omega + i0)$ where the T-matrix is $T(\omega) = \langle 0 | \hat{O}^{\dagger} \hat{O} | 0 \rangle$ with $\hat{O} = \frac{J}{2} (c_0, S_x + c_0, S_z)$ and $c_0 = \sum_k c_k$; is the electron operator on the first site of the Wilson chain. The low-temperature conductance $G = \frac{e^2}{2\pi} \int d\omega A(\omega) f(\omega) = \frac{e^2}{2\pi} \int d\omega A(\omega) f(\omega)$ is proportional to the spectral function, where $f(\omega) = 1/(e^{\beta\omega} + 1)$. The effects considered here are difficult to capture in a poor man's scaling approach due to the strong coupling and the many excited states involved. However, another useful guide to the full NRG results in this regime is the spin binding energy E , obtained by diagonalizing exactly the molecular Hamiltonian Eq. (1) coupled by exchange to a single conduction electron spin. This is similar to the first step of a NRG calculation and will be denoted as the zero-bandwidth model. The ground-to-excited-state gap E thus obtained follows the modulation of T_K by B_2 and H_z accurately, although the scales of E and T_K strongly differ. Apparently, for a sizable range of the relevant exchange strengths $J < W$ the zero-bandwidth estimate E is renormalized uniformly by the coupling to the remaining conduction band electrons. This estimate breaks down, when the modulation involves a suppression of T_K far below the scale of the magnetic splittings: then the renormalization becomes non-uniform and the variation may deviate from the NRG.

Kondo effect due to excited states tuned by QTM. We first consider the case of zero magnetic field. For integer spin this corresponds to an anticrossing: the eigenstates are paired to nearly degenerate states from the same subspace which are splitted by the transverse anisotropy. Consequently, as discussed above the Kondo effect is suppressed, resulting even in a dip in the spectral function, see below. In contrast, for half-integer spin many topological pairs are degenerate (crossing) due to time-reversal symmetry, see Fig. 1. The NRG converges to the spin-1/2 strong coupling fixed point, indicating a complete screening of the magnetic degrees of freedom. As shown in Fig. 2(a) the Kondo temperature shows an oscillatory dependence on B_2/D . The number of oscillations for $0 < B_2/D$ is $S - 1 = 2$. When decreasing the exchange coupling J the smallest peaks disappear

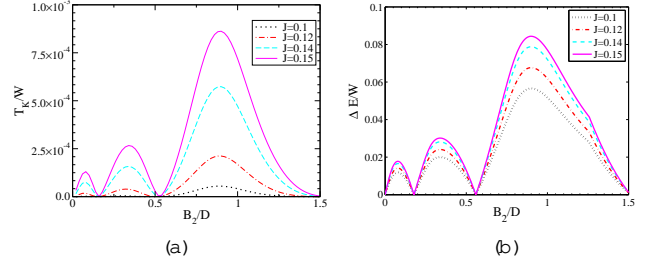


FIG. 2: Dependence of T_K on the transverse anisotropy B_2/D : (a) T_K from the full NRG calculation, (b) spin binding energy estimate E . Parameters: $S = 7/2$, $D = 5 \cdot 10^{-5}W$.

first, leaving only the monotonic increase of T_K up to the broad maximum centered at B_2/D in the limit where the magnetic excitations can be neglected [5]. The spin binding energy E captures this dependence on B_2/D , as shown in Fig. 2(b). Interestingly, we find that the nature of the ground state of the zero-bandwidth model changes with each oscillation which can in turn be related to an anticrossing of magnetic states on the SMM. For instance, for weak B_2/D near the lowest peak in Fig. 2(b) the highest excited Kramers doublets are strongly mixed into the zero-bandwidth model ground state. In contrast, for B_2/D near the highest peak in Fig. 2(b) the ground doublet dominates in the ground state. This demonstrates that the observed strong coupling Kondo fixed point in the NRG indeed originates from a screening of magnetic degrees of freedom involving excited magnetic states of the SMM. Which of these excited states are important depends on B_2/D .

Kondo spectroscopy of SMMs. We now focus on the most relevant case of fixed weak QTM (B_2/D) and vary the longitudinal magnetic field H_z . For any magnetic field values the spectral density shown in Figs. 3(a)–3(d) displays a zero-bias Kondo resonance. The corresponding many-body ground state found in the NRG at the strong coupling fixed point is non-degenerate. This peak is strongly modulated at avoided crossings of states from the same subspace at $H_z = D - 2k$ ($2k + 1$), $k = 1; 2; \dots$ for integer (half-integer) spin. As discussed above, this is related to the strong suppression of effective exchange couplings on the magnetic field scale B_2 near an anticrossing. In contrast, the spectral function varies smoothly at level crossings located at $H_z = D - 2k + 1$ ($2k$) for integer (half-integer). In this way the two scales D and B_2 can be identified in the magnetic field dependence of the linear conductance. For integer spin $S = 1$ the spectral function in Fig. 3(a) shows a dip for $H_z = 0$ (anticrossing of $j_l + i$ and $j_l + i$). At fields $H_z = B_2$ a Kondo peak is induced which reaches maximal height at $H_z = D$ (crossing of $j_l + i$ and $j_l - i$). This Kondo peak is subsequently suppressed and splitted due to the Zeeman level shifts, see Fig. 1. For half-integer spin $S = 3/2$ the zero-frequency peak at $H_z = 0$ in Fig. 3(b) is broadened with increasing H_z . This broadening is maximal at

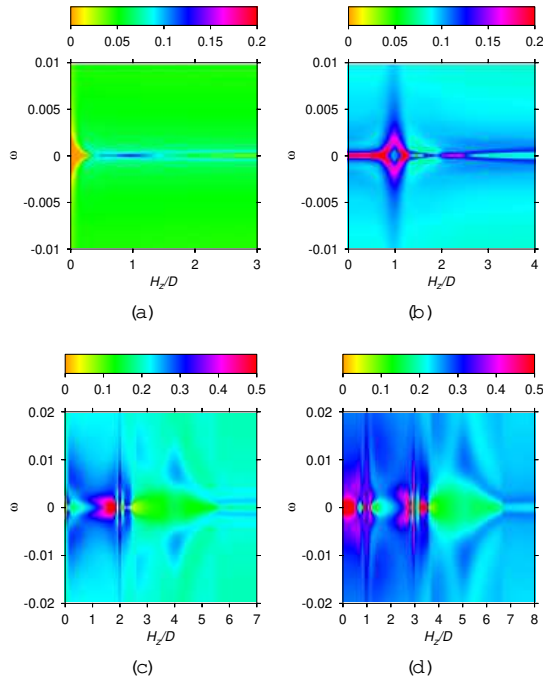


FIG. 3: (Color online) Spectral function, qualitatively equivalent to dI/dV_{bias} as function of H_z/D and frequency ω . (a) for smallest non-trivial integer spin $S = 1$, (b) half-integer spin $S = 3/2$, and (c) large integer $S = 3$, (d) half-integer spin $S = 7/2$. Parameters: $J = 0.15W$; $D = 5 \cdot 10^5 W$ and $B_z/D = 0.1$.

$H_z = D$ and is also captured by the H_z/D dependence of the spin-binding energy E (not shown). The full NRG result in addition shows a sharp dip superimposed on the broad peak at $H_z = D$ (anticrossing of $j_l + i$ and $j_l + i$). At this point the situation is very similar to the $S = 1$ case, provided one neglects the contribution of the low lying state $j_l + i$ and reduces the magnetic field by D , see Fig. 1. Indeed, increasing the field further to $H_z = 2D$, the Kondo effect reappears precisely as for $S = 1$ near $H_z = D$. For larger spin the physics is qualitatively the same: the spectral function in Figs. 3(c), 3(d) dis-

plays several dips of the Kondo peak close to each anti-crossing. The correspondence pointed out above is more general: the linear conductance of a SMM with spin S at magnetic field H_z corresponds qualitatively to that of a SMM with reduced spin $S - 1/2$ and reduced magnetic field $H_z - D$. This can be shown using the Hamiltonian Eq. (4) in the molecular eigenbasis. For fixed J the correspondence in the conductance is most obvious for subsequent S values. The conductance for spin S near $H_z = nD$ ($n = 1; 2; \dots; 2S - 1$) can even be compared with that for $S - n/2$ around zero-field by iterating n times, which we have checked. However, a clear correspondence appears only when J is properly adjusted.

Conclusion. Magnetic field Kondo transport spectroscopy can determine the absolute value of the spin and the magnetic parameters of a SMM in a transport junction. The strong Kondo effect in SMMs discussed in this work can be accessed experimentally by increasing the exchange coupling. In STM setups one can reduce the distance to the molecule, or change the molecular geometry by a bias-voltage pulse [19]. In 3-terminal measurements [2, 3] one can tune the exchange coupling with the gate voltage: $J/4 = J_g - V_g j$. In addition, both the charge- and spin-state can be changed by tuning the gate voltage to opposite sides of the charge degeneracy point $V_g = V_g$. If a single-electron transport current [6] is observed at this point c.f. [2, 3], S only changes by $1/2$. Then the predicted clear correspondence between the linear conductance for subsequent integer and half-integer spin values provides an additional check on the physics. Importantly, the spectroscopy can be done at temperatures above the energy scale of the magnetic splittings and requires only low magnetic fields which do not destroy the Kondo effect by Zeeman splittings. Finally, we have checked that small fixed transverse magnetic field perturbation does not destroy the reentrant behavior of the Kondo effect as the longitudinal field is varied.

We acknowledge P. Nozières, H. Park and H. van der Zant for discussions and financial support through the EU RTN Spintronics program HPRN-CT-2002-00302 and the FZ Jülich via the virtual institute IFM IT.

[1] D. Gatteschi and R. Sessoli, *Angew. Chem. Int. Ed.* **42**, 268 (2003), and references therein.
[2] H. Heersche, Z. de Groot, J. A. Folk, H. S. J. van der Zant, C. Romo-Wegeij, L. Zobbi, D. Barreca, E. Tondello, and A. Comia, *cond-mat/0510732*, *Phys. Rev. Lett.* (to be published).
[3] M.-H. Jo, J. E. Grose, M. M. Deshmukh, J. J. S. M. Rumberger, D. N. Hendrickson, J. R. Long, H. Park, and D. C. Ralph, *cond-mat/0603276*.
[4] G.-H. Kim and T.-S. Kim, *Phys. Rev. Lett.* **92**, 137203 (2004).
[5] C. Romo-Wegeij, M. R. Wegewij, W. Hofstetter, and H. Schoeller, *Phys. Rev. Lett.* **96**, 196601 (2006).

[6] C. Romo-Wegeij, M. R. Wegewij, and H. Schoeller, *Phys. Rev. Lett.* **96**, 196805 (2006).
[7] D. Goldhaber-Gordon, H. Shtrikman, D. Mahalu, D. Abusch-Magder, U. Meirav, and M. A. Kastner, *Nature (London)* **391**, 156 (1998).
[8] S. M. Cronenwett, T. H. Oosterkamp, and L. P. Kouwenhoven, *Science* **281**, 540 (1998).
[9] F. Simmel, R. H. Blick, J. P. Kotthaus, W. Wegscheider, and M. Büchler, *Phys. Rev. Lett.* **83**, 804 (1999).
[10] J. Schmid, J. Weis, K. Eberl, and K. v. Klitzing, *Phys. Rev. Lett.* **84**, 5824 (2000).
[11] W. G. van der Wiel, S. de Franceschi, T. Fujisawa, J. M. Elzerman, S. Tarucha, and L. P. Kouwenhoven, *Science*

- 289, 2105 (2000).
- [12] J. Park, A. N. Pasupathy, J. I. Goldsmith, C. Chang, Y. Yaish, J. R. Petta, M. Rinkoski, J. P. Sethna, H. D. Abruna, P. L. McEuen, et al., *Nature* 417, 722 (2002).
 - [13] W. Liang, M. P. Shores, M. Bockrath, J. R. Long, and H. Park, *Nature* 417, 725 (2002).
 - [14] L. I. Glazman and M. E. Raikh, *JETP Lett.* 47, 452 (1988).
 - [15] T. K. Ng and P. A. Lee, *Phys. Rev. Lett.* 61, 1768 (1988).
 - [16] K. G. Wilson, *Rev. Mod. Phys.* 47, 773 (1975).
 - [17] W. Hofstetter, *Phys. Rev. Lett.* 85, 1508 (2000).
 - [18] T. A. Costi, *Phys. Rev. Lett.* 85, 1504 (2000).
 - [19] V. Tancu, A. Deshpande, and S. W. Hla, *Nano Lett.* 6 (4), 820 (2006).